LETTERS
PUBLISHED ONLINE: 15 JUNE 2014 | DOI: 10.1038/NGEO2187

nature geoscience

Rejuvenation of Appalachian topography caused by subsidence-induced differential erosion

Lijun Liu*

In ancient orogens, such as the Appalachian Mountains in the eastern United States, the difference between the high and low points—topographic relief—can continue to increase long after the tectonic forces that created the range have become inactive. Climatic forcing[1] and mantle-induced dynamic uplift[2,3] could drive formation of relief, but clear evidence is lacking in the Appalachian Mountains. Here I use a numerical simulation of dynamic topography in North America, combined with reconstructions of the sedimentation history from the Gulf of Mexico[4], to show that rejuvenation of topographic relief in the Appalachian Mountains since the Palaeogene period could have been caused by mantle-induced dynamic subsidence associated with sinking of the subducted Farallon slab. Specifically, I show that patterns of continental erosion and the eastward migration of sediment deposition centres in the Gulf of Mexico closely follow the locus of predicted dynamic subsidence. Furthermore, pulses of rapid sediment deposition in the Gulf of Mexico[4] and western Atlantic[5] correlate with enhanced erosion in the Appalachian Mountains during the Miocene epoch, caused by dynamic tilting of the continent. The model predicts that such subsidence-induced differential erosion caused flexural-isostatic adjustments of Appalachian topography that led to the development of 400 m of relief and more than 200 m of elevation. I propose that dynamically induced continental tilting may provide a mechanism for topographic rejuvenation in ancient orogens.

Although it is well accepted that active tectonic forces created most orogenies on Earth[6], the topographic rejuvenation of ancient orogens long after tectonic activity ceased remains enigmatic. One such example is the Appalachians formed at the end of the Palaeozoic, where several studies reveal almost contemporaneous exhumation[1] and topographic relief growth[2,3] since the Mid-Miocene. One mechanism proposed for developing Miocene and younger Appalachian topography is climate forcing[1,7]. However, although there is a good correlation between late Cenozoic uplift of mountain ranges and the concurrent global glaciation[8], climate forcing (post 4 Ma (Myr ago)) does not explain the Appalachian topography development, which started no later than 10 Ma (refs 1–3). An alternative proposal is that mantle-induced dynamic uplift triggered the development of the relief the range has today[2,3].

Broad-scale mantle convective flow can generate temporally varying surface deformation, namely dynamic topography. The amount of deformation can be estimated by calculating buoyancy-induced mantle flow[9,10]. Such estimates, however, still exhibit considerable discrepancies[9–12] due to uncertainties in estimates of mantle buoyancy and viscosity structures, both important variables for calculating mantle flow. Among the various approaches for estimating mantle buoyancy, a promising one converts seismic anomalies to density, and this approach has been widely used in estimating vertical motion history of continents[10–13]. There is, however, still no consensus on the depth-dependence of the mantle viscosity profile[12–16].

Figure 1 presents three calculations of the change of dynamic topography over the eastern United States since 10 Ma using endmember estimates of mantle buoyancy and viscosity structures (see Methods and Supplementary Information for more details). Notably, these calculations do not all yield the same vertical motion for the northeastern United States—Cases 1 and 2 show subsidence whereas Case 3 shows uplift. This highlights the debates on the vertical motion of offshore New Jersey[11,12], which partly reflects the uncertain interpretation of passive-margin mantle seismic structures. Nevertheless, all three calculations show a clear pattern of dynamic subsidence along the Appalachians, so it is unlikely that Appalachian topographic rejuvenation since the Mid-Miocene was driven by dynamic uplift. In fact, the only case predicting some local uplift (Fig. 1c; ref. 12) would suggest more topographic relief development in the central than in the southern Appalachians, opposite to the distribution of relief observed[2,3]. To predict a meaningful dynamic topography history, a model must be consistent not only with present-day observations but also with constraints from the geological past[10,13]. Cases 1 and 2 (Fig. 1a,b) both satisfy these conditions, and show similar long wavelength dynamic topography evolution during the Cenozoic. For the rest of the discussion, I will refer to the Case 1 calculation.

An understanding of the relationship between dynamic subsidence and orogenic deformation may come from studying the sedimentation and subsidence history of passive-margin basins surrounding a continent[17,18]. The Gulf of Mexico (GOM), a passive-margin basin that initiated in the Jurassic, spans a similar longitude range as does the eastern United States (Fig. 2a). During the Cenozoic, the GOM accumulated immense amounts of sediments, sourced mainly by erosion of continental North America[18–21]. This accumulation history records three particularly rapid depositional episodes[18]: Palaeocene (65–50 Ma), Miocene (20–10 Ma) and Quaternary (< 2 Ma), with a rate of deposition reaching as high as 1.5×10^5 km^3 Myr^{-1} (Fig. 2b). These episodes are characterized by sand-rich sediments, indicative of high rates of continental erosion and transportation[18,20]. Figure 2c shows the depth and thickness of sedimentary strata by age along a basin-wide SW–NE profile within the GOM, compiled from a few earlier studies[19–21]. Based on thicknesses of the Palaeogene, Neogene, and Quaternary strata, we calculated residual subsidence (flexural + dynamic subsidence) profiles assuming isostatic equilibrium[10] (Fig. 2c). Geographically, the three age groups of sediments are offset from each other, clearly showing a progressive eastward migration of the depocentre over time (Fig. 2c). This migration indicates a basin-scale dynamic process.

Predicted dynamic topography along the same profile (Fig. 2d) shows a remarkably similar eastward migration to that seen in the GOM residual subsidence. Magnitudes of these two subsidence

Department of Geology, University of Illinois at Urbana-Champaign, Champaign, Illinois 61820, USA. *e-mail: ljliu@illinois.edu

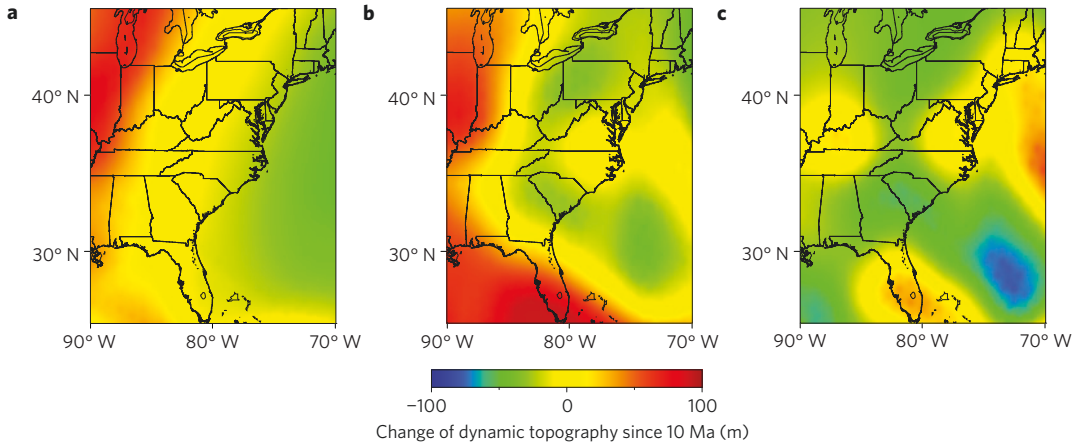

Figure 1 | Changes of dynamic topography since 10 Ma using tomography-converted buoyancy structures. The three calculations are based on simple inversions of mantle flow (Supplementary Information). **a**, Adopting a buoyancy and viscosity structure consistent with ref. 13. **b**, Adopting a buoyancy from ref. 15 and a viscosity consistent with the Late Cretaceous western interior seaway subsidence. **c**, Adopting a buoyancy from ref. 15 and a viscosity similar to ref. 12.

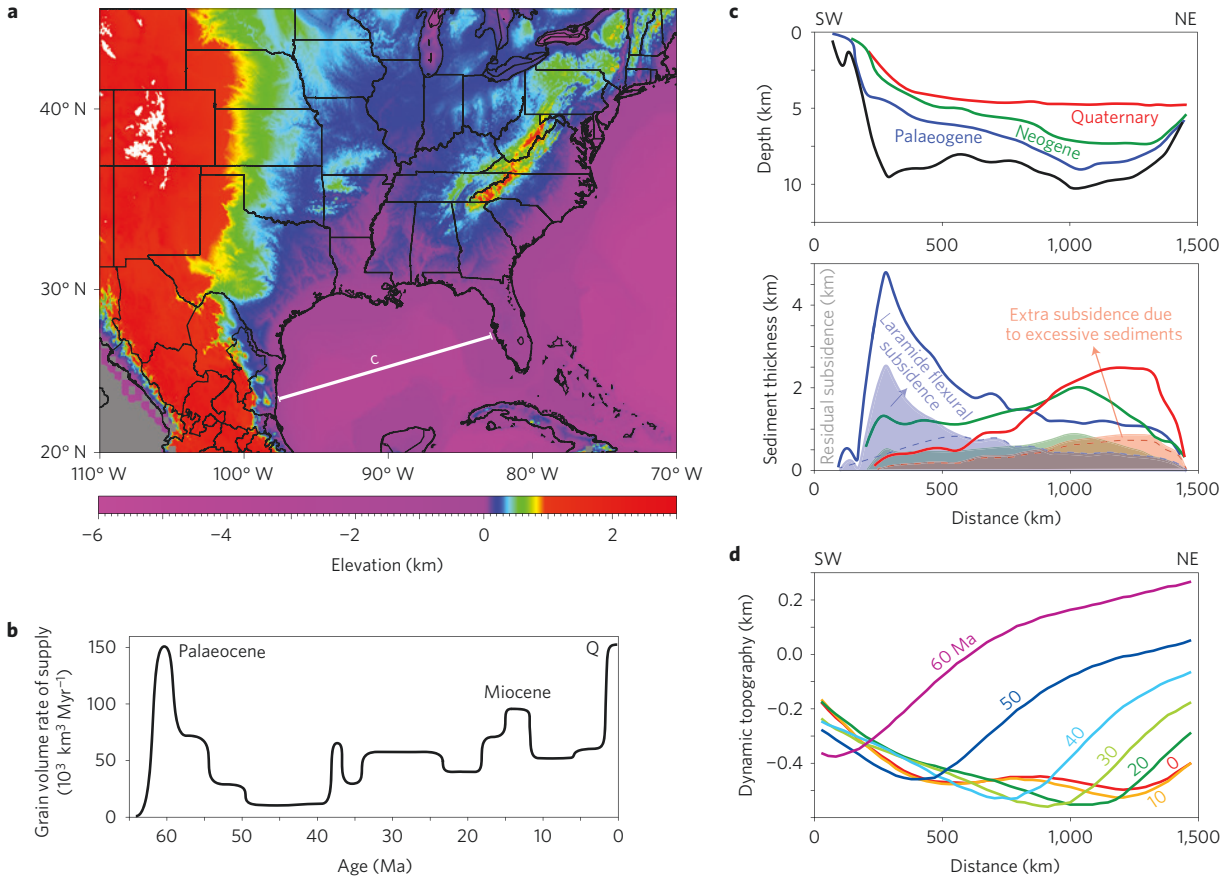

Figure 2 | Temporal and spatial variations of Gulf of Mexico sedimentation. a, Topography of eastern North America and the location of a SW-NE profile within the Gulf of Mexico (GOM). **b**, Rate of sediment accumulation within the GOM during the Cenozoic, modified from ref. 18. **c**, Depths and thicknesses of three consecutive sediment strata along the profile shown with a white line in **a**, with coloured lines marking the strata surfaces in both the upper and lower plots, and the black line denoting the bottom of the Palaeogene stratum. Also plotted are inferred residual subsidence (coloured shaded areas; that is, flexural + dynamic subsidence) from these strata, Laramide flexural subsidence in the western Gulf (above blue dashed line), and possible Quaternary additional subsidence due to excessive sediment loading in eastern Gulf (above red dashed line). **d**, Predicted Cenozoic dynamic topography evolution along the same profile at intervals of ten million years (following refs 13,22).

patterns also agree for most geologic periods: Palaeogene versus 60–30 Ma, Neogene versus 30–10 Ma, and Quaternary versus 10–0 Ma, respectively. As suggested by earlier studies based on local data[10,13,22,23], a continent-wide eastward shifting subsidence pattern should have resulted from the westward motion of North America relative to former Farallon slabs at depths. The correlation of

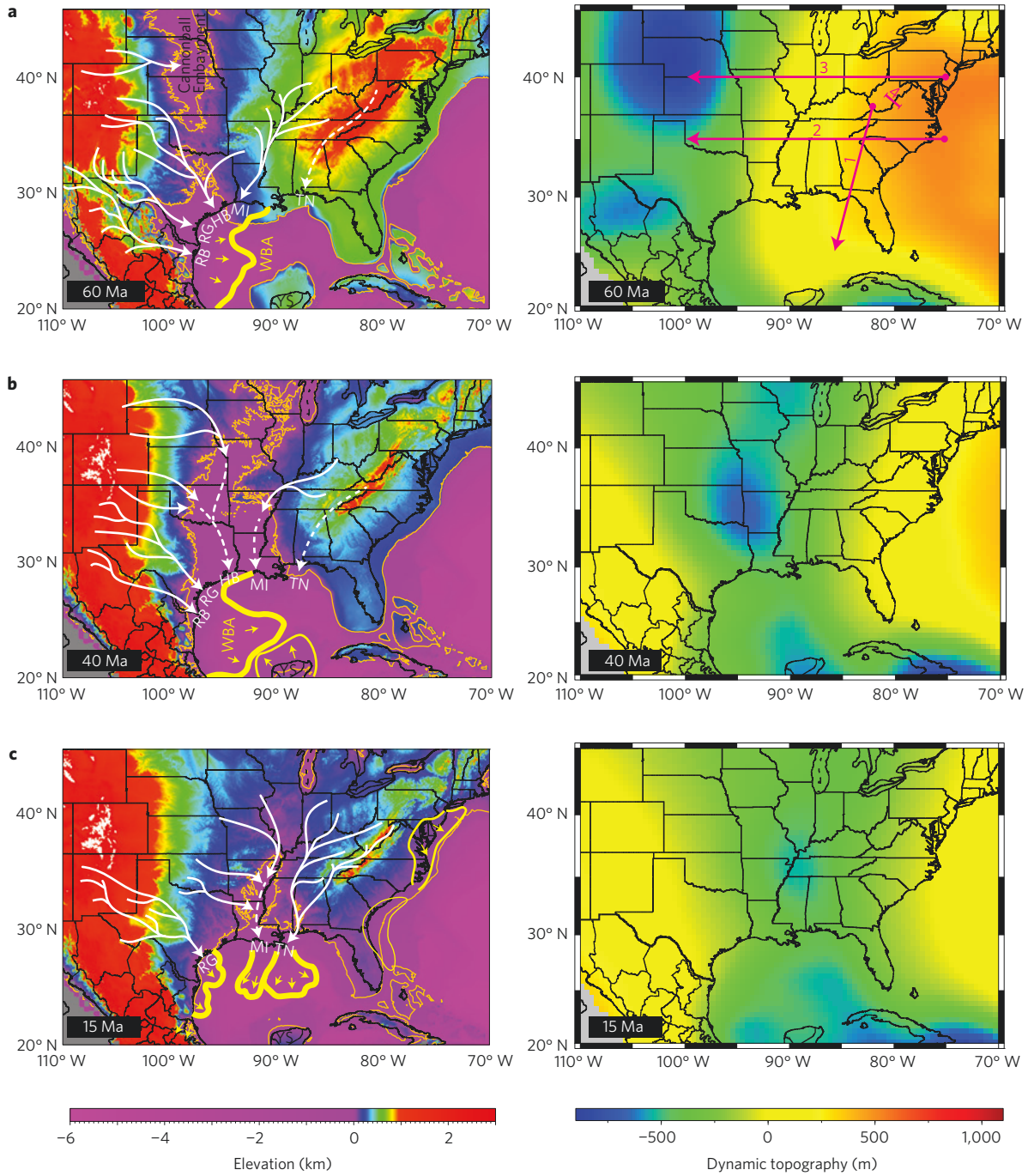

Figure 3 | Palaeotopography maps of the eastern United States. a–c, Snapshots at 60 Ma (**a**), 40 Ma (**b**) and 15 Ma (**c**) where both the palaeosurface (left) and dynamic topographies (right) are shown. Overplotted on the palaeotopography are palaeoriver systems from ref. 18, major GOM depositional episodes from ref. 24, and Atlantic Miocene depositional episodes from ref. 5; brown-coloured lines represent palaeoshorelines; the thicknesses of the yellow-coloured strata outlines are proportional to their total volumes. The four profile lines shown in **a** (right) are used in Fig. 4. RB, Rio Bravo; RG, Rio Grande; HB, Houston Brazos; MI, Mississippi; TN, Tennessee; WBA, Western Basin Apron; YS, Yucatan Scarp.

modelled dynamic subsidence with the GOM sedimentary records (Fig. 2c,d), for the first time, provides direct observational evidence for this prediction. Among the three sedimentation episodes (Fig. 2b,c), the thick Palaeogene sedimentary wedge within western GOM was attributed to flexural subsidence from the Laramide orogeny in Mexico[19], but the long wavelength (>500 km) subsidence is probably due to dynamic topography. Space for the voluminous Quaternary deposition in eastern Gulf accompanying the latest Cenozoic glaciation[8] could be partly a result of excessive sediment loading. However, it is worth noting that neither of these factors would have caused the temporal migration of depocentres within the GOM.

The next step is to identify the source region of major Cenozoic GOM deposits, which involves a detailed analysis of numerous seismic profiles and well data[19–21,24]. I constructed a series of palaeotopography maps by correcting the effects of dynamic topography from the present-day surface topography, but without removing the existing sediments (Fig. 3). During the Late Palaeocene, the western Gulf received the first major Cenozoic sediment influx that formed the western basin submarine apron

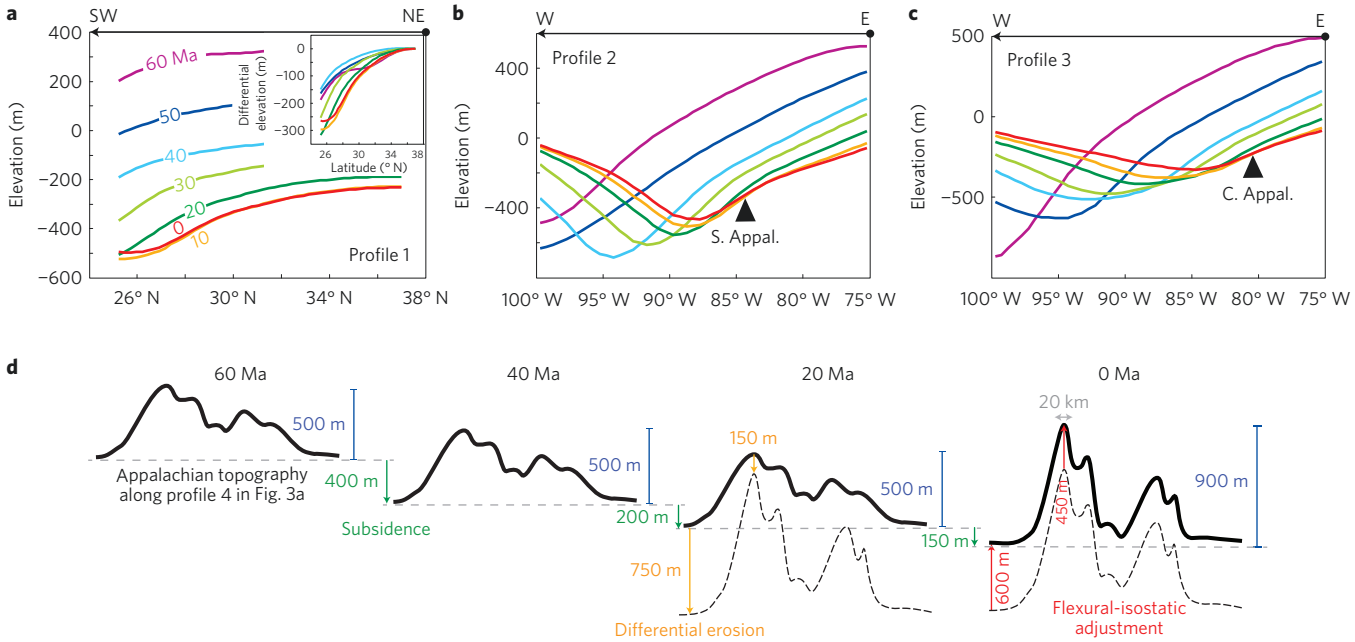

Figure 4 | Surface elevation changes caused by dynamic topography and flexural-isostatic adjustment. a–c, Temporal variation of dynamic topography along profiles 1–3 indicated in Fig. 3a. The inset plot in **a** shows the relative topography from the profile's north end, approximating evolving surface slopes. S. Appal., Southern Appalachians; C. Appal., Central Appalachians. **d**, A schematic representation of Cenozoic Appalachian topography evolution along profile 4. This includes a continuous baseline subsidence from 60 to 20 Ma, followed by a major topographic rejuvenation where sharpened and elevated mountain peaks form as a result of differential erosion. The calculation of flexural-isostatic adjustment is presented in the Methods section.

(WBA; Fig. 3a). Although this deposition is qualitatively attributed to Laramide-induced flexural loading[19,24], the topography around 60 Ma featuring a southern Texas–northern Mexico depression due to dynamic subsidence illustrates how regional surface erosion could be enhanced by steepened channel slopes of the ancient Rio Bravo and Rio Grande rivers[18] (Fig. 3a). The North American topography back then is characterized by a NS-oriented central trough, separating the steep western continent from the flat eastern part. The map reproduces the presence of the marine Cannonball Embayment, which extends south from Canada across the Dakotas[18] (Fig. 3a). This configuration also suggests the dominant sediment source to be the western continental interior, consistent with the abundance of volcanic clasts in basin sediments[24].

Palaeotopography during the Early to Middle Eocene features an extensive south-trending lowland, due to still significant surface subsidence (> 500 m) in the Mid-continent (Fig. 3b). This explains the extensive flooding of the Mississippi Embayment[18] and the presence of broad fluvial and deltaic deposition systems across the central Gulf margin[24]. This time interval represents a slow depositional period inside the GOM (Fig. 2b), perhaps because sediments were collected within the lowland channel instead of being transported into the Gulf. On the other hand, the eastward shift of the subsidence centre within the GOM is linked to the observed eastward progression of the WBA into the central Gulf during the early Eocene[24]. Formation of a concurrent mudflow deposit on the northern side of the Yucatan scarp[24] seems to reflect the same local maximum subsidence in the central GOM (Fig. 3b).

The amplitude of dynamic subsidence declined further into the Miocene, raising the Midcontinent above sea level (Fig. 3c). Meanwhile, the eastward migration of dynamic subsidence further lowered the eastern continental interior and northeastern GOM as the long-lasting southern subsidence centre moved northeast (Fig. 3a–c). As a result, the ancestral Tennessee River surpassed the ancestral Mississippi River in terms of the sediment volume that it delivered into the Gulf[18]. This is further reflected in a sharp transition from a previous carbonate-dominated system to the accumulation of coarse-grained clastic deposits in the northeastern GOM and adjacent onshore areas[24]. The Miocene also marks the age when these two river systems started to dominate the sediment supply within the entire GOM (Fig. 2b). This situation eventually led to the formation of widespread central- to eastern-basin deltaic and submarine fan systems prograding into and filling the region of maximum dynamic subsidence (Fig. 3c). This corresponds to a prominent peak in the total volume rate of deposition inside the GOM (Fig. 2b). Meanwhile, an increase of sedimentation rate also occurred along the eastern Atlantic margin[5] (Fig. 3c).

The synchroneity between enhanced GOM deposition (via dynamic subsidence) and Appalachian relief development[1–3] during the Miocene strongly suggests a causal relationship between the two events. This proposal is compatible with a recent reconstruction of major river systems[18], which shows that the ancestral Tennessee fluvial system transported materials from the western and southern Appalachians into the GOM (Fig. 3). Of note, even though rivers eroding the eastern Appalachians led to a prominent increase in sedimentation along the eastern Atlantic margin (Fig. 3c), the fact that a much larger volume of sediments deposited in the northeastern GOM (refs 18,21; Fig. 2b) than the Atlantic[5] (Fig. 3c) emphasizes the stronger denudation over the southern rather than the central Appalachians[2,3]. Therefore, the eastward propagating dynamic subsidence (Figs 2 and 3) should have played an important role from enhancing regional erosion to regulating sediment transport into the GOM.

The topographic gradient of drainage systems represents an important factor affecting the tectonic erosion rate[25,26]. Spatially, the pattern of dynamic subsidence parallels the orientation of the Appalachians (Fig. 3), consistent with its NS-synchronized topographic rejuvenation[1–3]. The temporal change of dynamic topography along a NE–SW profile from the southern Appalachians to the northeastern GOM demonstrates a monotonic drop of surface elevation until ~10 Ma (Fig. 4a), and a rapid increase of surface slope starting ~30 Ma and peaking between 20 and 10 Ma (Fig. 4a

inset plot). Similarly, the topographic gradient on the western flank of the southern Appalachians (35° N) reached a maximum at ~20 Ma whereas that of the eastern flank reached a maximum between 20 and 10 Ma (Fig. 4b). The central Appalachians (40° N) experienced a rapid regional tilting that raised the western flank at around the Mid-Miocene (Fig. 4c). This continental-scale topographic tilting event should have greatly enhanced erosion in the Appalachian's NS Central Valley and its west and east flanks (Figs 3 and 4). Effectively, this movement had the same consequence as a base-level fall of a river[27]—just like a base-level fault increases river-incision rates even without uplift of the headwaters upstream, the base-level drop caused an increased erosion rate due to continental tilting even without uplift of the mountain range.

The past Appalachian mountain topography can be estimated from the GOM sediment record[28] (Fig. 2b) and the dynamic topography history (Fig. 3). Calculations restoring the Miocene GOM sediments on land suggest an average Appalachian relief growth of ~400 m due to flexural-isostatic adjustment, given the observed differential erosion rates[2,3] (Methods and Fig. 4d). To estimate the elevation change over time, we further consider dynamic topography, which suggests a continuous large-scale subsidence at a rate of ~20 m Myr^{-1} in the Palaeogene that reduced to ~2 m Myr^{-1} in the Miocene (Figs 3 and 4); a net elevation gain of at least 200 m occurred at the mountain peaks. This work yields a model of Cenozoic topographic evolution in the Appalachians: a regional scale subsidence with little relief variation began at 60 Ma and continued until 20 Ma; then there was a topographic rejuvenation, with significant increases in both surface relief and maximum elevation towards the present day, sharpening the mountain range (Fig. 4d). This cause of uplift should be taken into account when evaluating the development of renewed topographic relief over ancient orogenic belts.

Methods

Calculation of dynamic topography. I use geodynamic models with data assimilation to estimate the history of dynamic topography over North America. More details about the numerical modelling can be found in the Supplementary Methods. Mantle buoyancy is converted from seismic velocity anomalies using different observational constraints (Supplementary Fig. 1a). I use two endmember mantle viscosity profiles to estimate the possible magnitude of dynamic topography (Supplementary Fig. 1b). Among the three representative cases presented in Fig. 1, I use different combinations of endmember buoyancy and viscosity estimates (Supplementary Fig. 1): Case 1 (Fig. 1a) assumes the same seismic-to-density conversion as in ref. 13 and a 20-fold viscosity increase across the upper–lower mantle interface, both constrained by the subsidence history of the Cretaceous Western Interior Seaway[13]; Case 2 (Fig. 1b) uses a density structure from a joint seismic-geodynamic inversion[15] and a corresponding viscosity structure predicting a similar dynamic topography to the Cretaceous subsidence history in ref. 13; Case 3 (Fig. 1c) is the same as Case 2 but with a weaker asthenosphere and stronger lower mantle (a 500-fold maximum viscosity increase with depth[12]). Given the wide parameter range, these calculations should provide a good coverage on the possible histories of dynamic topography evolution over the eastern United States.

Restoration of Appalachian topography since the Miocene. I estimate the volume of sediment originating from the eastern United States since 20 Ma to be at least 7.5×10^5 km^3 (Fig. 2b), and the area of corresponding fluvial systems (Fig. 3c) to be $10° \times 10°$ in latitude and longitude or 10^6 km^2 equivalent. These convert to a mean erosion thickness of 750 m since the Miocene, probably representing a lower limit estimate. Recent studies[2,3] suggest a much lower erosion rate (by a factor of five) at highest elevations among the Appalachians, implying a net erosion of Appalachian mountain peaks by only 150 m since the Miocene, with a 600 m differential erosion relative to the surrounding continental surface.

The isostatic rebound of the crust–mantle interface during erosion can be estimated as $h = \rho_c / \rho_m \cdot H_{\text{erosion}}$. Assuming crust density ρ_c (2.8 g cm^{-3}) and mantle density ρ_m (3.3 g cm^{-3}) gives a rebound of 636 m for an erosion thickness (H_{erosion}) of 750 m. Consequently, this suggests a 114 m net subsidence of the regional surface topography.

Finally, I calculate the flexural support of individual Appalachian mountain peaks. The typical widths of the highest peaks are 20–30 km (for example, Figs 2 and 4d), much smaller than the lithospheric flexural thicknesses (100–120 km; ref. 29). The amount of flexural compensation of these peaks is calculated by[30]:

$$w = \frac{\rho_c H_L}{\rho_m - \rho_s}\left[1 - \exp\left(-\frac{L}{\alpha}\right)\cos\left(\frac{L}{\alpha}\right)\right]$$

where ρ_s (2.3 g cm^{-3}) is the sediment density, H_L (600 m) is the load height or thickness of differential erosion, L (20 km) is the load width, and α (200 km: ~2× elastic thickness) is the characteristic wavelength of the flexural topography. This calculation suggests that the local compensation of a 600-metre-height surface load over a 20 km-wide mountain peak is 167 m.

Combining the differential erosion and flexural compensation, we find that a narrow mountain peak would grow by $(750 - 150) - 167 = 433$ m in relief. Combining this relief growth with total surface subsidence (both isostatic and dynamic), we estimate the net elevation gain of the highest mountain peaks to be $433 - 114 - 50 = 269$ m. In conclusion, during the Miocene erosion, both the relief and elevation of Appalachian mountain peaks will grow significantly.

Received 19 December 2013; accepted 16 May 2014; published online 15 June 2014

References

1. Boettcher, S. S. & Milliken, K. L. Mesozoic–Cenozoic unroofing of the Southern Appalachian Basin: Apatite fission track evidence from middle Pennsylvanian sandstones. *J. Geol.* **102,** 655–663 (1994).
2. Miller, S. R., Sak, P. B., Kirby, E. & Bierman, P. R. Neogene rejuvenation of central Appalachian topography: Evidence for differential rock uplift from stream profiles and erosion rates. *Earth Planet. Sci. Lett.* **369–370,** 1–12 (2013).
3. Gallen, S. F., Wegmann, K. W. & Bohnenstiehl, D. R. Miocene rejuvenation of topographic relief in the southern Appalachians. *GSA Today* **23,** 4–10 (2013).
4. Galloway, W. E., Whiteaker, T. L. & Ganey-Curry, P. History of Cenozoic North American drainage basin evolution, sediment yield, and accumulation in the Gulf of Mexico basin. *Geosphere* **7,** 938–973 (2011).
5. Poag, C. W. & Sevon, W. D. A record of Appalachian denudation in postrift Mesozoic and Cenozoic sedimentary deposits of the US middle Atlantic continental margin. *Geomorphology* **2,** 119–157 (1989).
6. Molnar, P. & Lyon-Caen, H. Some simple physical aspects of the support, structure, and evolution of mountain belts. *GSA Spec.* **218,** 179–207 (1988).
7. Whipple, K. X. The influence of climate on the tectonic evolution of mountain belts. *Nature Geosci.* **2,** 97–104 (2009).
8. Zhang, P., Molnar, P. & Downs, W. R. Increased sedimentation rates and grain sizes 2-4 Myr ago due to the influence of climate change and erosion rates. *Nature* **410,** 891–897 (2001).
9. Lithgow-Bertelloni, C. & Richards, M. A. The dynamics of Cenozoic and Mesozoic plate motions. *Rev. Geophys.* **36,** 27–78 (1998).
10. Heine, C., Müller, R. D., Sterinberger, B. & Torsvik, T. H. Subsidence in intracontinental basins due to dynamic topography. *Phys. Earth Planet. Inter.* **171,** 252–264 (2008).
11. Spasojevi, S., Liu, L., Gurnis, M. & Muller, R. D. The case for dynamic subsidence of the United States east coast since the Eocene. *Geophys. Res. Lett.* **35,** L08305 (2008).
12. Moucha, R. *et al.* Dynamic topography and long-term sea-level variations: There is no such thing as a stable continental platform. *Earth Planet. Sci. Lett.* **271,** 101–108 (2008).
13. Liu, L., Spasojević, S. & Gurnis, M. Reconstructing Farallon plate subduction beneath North America back to the Late Cretaceous. *Science* **322,** 934–938 (2008).
14. Steinberger, B. & Calderwood, A. R. Models of large-scale viscous flow in the Earth's mantle with constraints from mineral physics and surface observations. *Geophys. J. Int.* **167,** 1461–1481 (2006).
15. Simmons, N. A., Forte, A. M. & Grand, S. P. Joint seismic, geodynamic and mineral physical constraints on three-dimensional mantle heterogeneity: Implications for the relative importance of thermal versus compositional heterogeneity. *Geophys. J. Int.* **177,** 1284–1304 (2009).
16. Paulson, A., Zhong, S. & Wahr, J. Inference of mantle viscosity from GRACE and relative sea level data. *Geophys. J. Int.* **171,** 497–508 (2007).
17. Steckler, M. S. & Watts, A. B. Subsidence of Atlantic-type continental margin off New York. *Earth Planet. Sci. Lett.* **41,** 1–13 (1978).
18. Galloway, W. E., Whiteaker, T. L. & Ganey-Curry, P. History of Cenozoic North American drainage basin evolution, sediment yield, and accumulation in the Gulf of Mexico basin. *Geosphere* **7,** 938–973 (2011).
19. Feng, J., Buffler, R. T. & Kominz, M. A. Laramide orogenic influence on late Mesozoic–Cenozoic subsidence history, western deep Gulf of Mexico basin. *Geology* **22,** 359–362 (1994).

20. Peel, F. J., Travis, C. J. & Hossack, J. R. Genetic structural provinces and salt tectonics of the Cenozoic offshore US Gulf of Mexico: A preliminary analysis. *AAPG Mem.* **65,** 153–175 (1995).
21. Galloway, W. E. *Sedimentary Basins of the World* Ch. 15 (Elsevier, 2008).
22. Spasojevic, S., Liu, L. & Gurnis, M. Adjoint models of mantle convection with seismic, plate motion, and stratigraphic constraints: North America since the Late Cretaceous. *Geochem. Geophys. Geosyst.* **10,** Q05W02 (2009).
23. Liu, S., Nummendal, D. & Liu, L. Migration of dynamic subsidence across the Late Cretaceous United States Western Interior Basin in response to Farallon plate subduction. *Geology* **39,** 555–558 (2011).
24. Galloway, W. E., Ganey-Curry, P. E., Li, X. & Buffler, R. T. Cenozoic depositional history of the Gulf of Mexico basin. *AAPG Bull.* **84,** 1743–1774 (2000).
25. Duvall, A., Kirby, E. & Burbank, D. Tectonic and lithologic controls on bedrock channel profiles and processes in coastal California. *J. Geophys. Res.* **109,** F03002 (2004).
26. Willett, S. D. Orogeny and orography: The effects of erosion on the structure of mountain belts. *J. Geophys. Res.* **104,** 28957–28981 (1999).
27. Reinhardt, L. J., Bishop, P., Hoey, T. B., Dempster, T. J. & Sanderson, D. C. W. Quantification of the transient response to base-level fall in a small mountain catchment: Sierra Nevada, southern Spain. *J. Geophys. Res.* **112,** F03S05 (2007).
28. Hay, W. W., Shaw, C. A. & Wold, C. N. Mass-balanced paleogeographic reconstructions. *Geol. Rundsch.* **78,** 207–242 (1989).
29. Karner, G. D. & Watts, A. B. Gravity anomalies and flexure of the lithosphere at mountain ranges. *J. Geophys. Res.* **88,** 10419–10477 (1983).
30. Angevine, C. L., Heller, P. L. & Paola, C. *Quantitative Sedimentary Basin Modeling* 36–58 (Continuing Education Course Notes No. 32, AAPG, 1990).

Acknowledgements

I thank J. Bennett for helping to collect data on the GOM sedimentary strata. This paper benefits from discussions with S. Marshak, W. Guenthner, W. Galloway, P. Heller and W. Hay. The calculations are performed on the TACC supercomputer Stampede under the XSEDE allocation EAR130036.

Additional information

Supplementary information is available in the online version of the paper. Reprints and permissions information is available online at www.nature.com/reprints.

Competing financial interests

The author declares no competing financial interests.